AIAA JOURNAL
Vol. 41, No. 11, November 2003

Efficient High-Order Frequency Interpolation of Structural Dynamic Response

Christophe Lecomte,* J. Gregory McDaniel,† Paul E. Barbone,‡ and Allan D. Pierce§
Boston University, Boston, Massachusetts 02215

A method is presented for interpolating structural dynamic response within a finite frequency band. It is based on a condensation of the equations of motion using the response vectors at interpolation points as a basis. This basis set naturally aligns itself with the eigenvectors whose eigenvalues lie inside the band, resulting in a small condensed model that yields the interpolated response. Combining the Sylvester law of inertia with eigenvalue analysis of the condensed system indicates when the condensation captures the eigenvalues that lie in the band of interest. The high accuracy of the interpolation results from a combination of features: an accurate estimation of eigenvalues and eigenvectors as well as matching the value and slope of the displacement vector projected on the force vector.

Nomenclature

$\boldsymbol{A}$	=	system matrix defined as $\boldsymbol{K} - \lambda\boldsymbol{M}$
c	=	set containing indices to a collection of eigenpairs
colsp($\boldsymbol{T}$)	=	column space of $\boldsymbol{T}$
diag($\boldsymbol{v}$)	=	diagonal matrix whose diagonal elements are the elements of the vector $\boldsymbol{v}$
eig($\boldsymbol{T}$)	=	set of eigenvalues of $\boldsymbol{T}$
$\boldsymbol{f}$	=	force vector
$\boldsymbol{g}$	=	condensed force vector
$\boldsymbol{K}$	=	stiffness matrix
$\boldsymbol{K}_T$	=	condensed stiffness matrix
$\mathcal{K}_k(\boldsymbol{A}, \boldsymbol{b})$	=	Krylov space defined as colsp($\boldsymbol{b}, \boldsymbol{A}b, \ldots, A^{k-1}b$)
l, i, u	=	sets containing indices to lower, interior, and upper eigenpairs
M	=	number of forced response vectors
$\boldsymbol{M}$	=	mass matrix
max(S)	=	maximum element in the set S
N	=	number of degrees of freedom
r	=	residual in forced-response problem
r_M	=	residual in eigenvalue problem
$\boldsymbol{x}$	=	forced-response vector
$\boldsymbol{T}$	=	mass-orthonormal transformation matrix
$\boldsymbol{\Lambda}$	=	diagonal matrix of eigenvalues
λ	=	frequency parameter defined as $\lambda = \omega^2$
λ_c	=	center frequency of eigenvalue collection
$\lambda_{\min}, \lambda_{\max}$	=	minimum and maximum of frequency parameter
λ_n	=	nth eigenvalue
$\lambda_{n,\min}, \lambda_{n,\max}$	=	lower and upper bounds on the nth eigenvalue estimate
$\tilde{\lambda}_n$	=	approximation of the nth eigenvalue
$\Sigma\boldsymbol{x}_q$	=	summation over eigenpairs in set q
$\boldsymbol{\phi}_n$	=	nth eigenvector
$\tilde{\boldsymbol{\phi}}_n$	=	approximation of the nth eigenvector
$\boldsymbol{\psi}_n$	=	nth eigenvector of the condensed problem
ω	=	forcing circular frequency

Subscripts

m	=	forced-response index
max	=	maximum value
min	=	minimum value
n	=	eigenpair index

Superscript

(k)	=	interpolation point index

Received 27 September 2002; revision received 17 April 2003; accepted for publication 7 May 2003.

*Graduate Research Assistant, Aerospace and Mechanical Engineering Department, 110 Cummington Street.

†Associate Professor, Aerospace and Mechanical Engineering Department, 110 Cummington Street; jgm@bu.edu. Member AIAA.

‡Associate Professor, Aerospace and Mechanical Engineering Department, 110 Cummington Street.

§Full Professor, Aerospace and Mechanical Engineering Department, 110 Cummington Street. Senior Member AIAA.

Introduction

ENGINEERS often use finite element models to predict the steady-state vibrational responses of structures. In the quest for ever more accurate simulations, models tend to be as large as available computational resources will allow. As a result, the typical cost (waiting time) of computing the response at a single frequency is barely tolerable, whereas the cost of predicting the response at many frequencies is extraordinarily high.

This paper presents a method called "forced-response condensation," which has been developed to reduce significantly the computational cost of predicting the frequency response of a structure, or alternatively, to increase greatly the accuracy of the prediction for a fixed investment of computational resources. Numerical evidence of the promise of the method was presented earlier.[1] The present paper is intended to establish the analytical foundations of the method and to describe its expected accuracy.

Forced-response condensation is based on reinterpolating a traditionally predicted frequency-response curve in an efficient manner. Standard interpolation methods involve fitting polynomial functions to data points, which in this context are responses computed at a finite number of frequencies. For undamped or lightly damped structures simple linear interpolation between adjacent points will not reveal resonances unless the response has been sampled near them. To ensure that resonances are not missed, in that case, the number of sampled frequencies must be large. Padé approximations[2] overcome some of these difficulties by matching derivatives of the transfer function with rational functions. Explicit Padé approximations however are limited to rather small sizes of reduced models.[3] Their utility is limited, therefore, to treating relatively small frequency bands.

Still other interpolation methods are based on constructing and solving reduced-order systems derived directly from the complete system. Though not traditionally described as interpolation methods, these include Guyan reduction,[4] condensation model reduction,[5–7] Krylov projection methods,[8–11] and a variety of

methods collectively referred to as model-reduction methods.[12,13] Many of these methods approximate the response as a linear combination of basis vectors within the Ritz approximation strategy, with the number of basis vectors being much smaller than the model size. Substitution of this approximation into the matrix equation of motion results in a much smaller system. The choice of basis vectors distinguishes between methods.

The proposed method also approximates the response using a subset of basis vectors. Here, the basis vectors are chosen to be precomputed response vectors at a relatively small number of frequencies within the frequency band of interest. This forced-response condensation favors the preservation of interior eigenpairs, each eigenpair consisting of an eigenvalue and its associated eigenvector, and therefore captures most of the response features in the band. This fact was recently used by McDaniel et al.[14] and Ruhe[15] as the basis of an eigenvalue algorithm. Exterior eigenpairs are not favored for preservation; however, the effects of the exterior eigenpairs on the response in the band are approximated by a much smaller set of eigenpairs in the condensed model.

By combining the Sylvester law of inertia[16] and known eigenvalue bounds, the proposed method indicates when all of the interior eigenpairs are accurately represented in the interpolated response. The theorem is used to calculate the number of eigenvalues that lie in the band, and this number is compared to the number of accurate in-band eigenvalues contained in the condensed model. The accuracy of each eigenpair is assessed by combining previously published error bounds in a new way. As a result, one can check that the interpolated response will contain only peaks near the actual ones, and that no peak is missed.

Problem Statement

With the neglect of damping, frequency-domain finite element models of linear vibrating structures result in matrix equations of the form

$$\boldsymbol{A}(\lambda)\boldsymbol{x}(\lambda) = (\boldsymbol{K} - \lambda\boldsymbol{M})\boldsymbol{x}(\lambda) = \boldsymbol{f} \tag{1}$$

The mass matrix $\boldsymbol{M}$ and stiffness matrix $\boldsymbol{K}$ are sparse and have dimension $N \times N$, where N is large. Furthermore, we shall assume that the mass matrix is symmetric positive definite and the stiffness matrix is symmetric positive semidefinite. The frequency parameter is equal to the square of the circular forcing frequency $\lambda = \omega^2$, whereas both matrices as well as the force vector $\boldsymbol{f}$ are assumed independent of frequency. The present paper uses the convention that boldfaced uppercase variables represent matrices and boldfaced lowercase variables represent column vectors.

We seek estimates of the forced response $\boldsymbol{x}(\lambda)$ in the frequency band specified by $\lambda_{\min} \le \lambda \le \lambda_{\max}$. Even when iterative solvers are used, the evaluation of the forced response at a fixed frequency is very expensive because of the size of the problem. Therefore, engineers often compute the solution at a relatively small set of points denoted here by $\lambda = \sigma_m$ $(m = 1, \ldots, M)$ to get an idea of the general behavior of the system. Each response vector is found by solving the equation

$$(\boldsymbol{K} - \sigma_m\boldsymbol{M})\boldsymbol{x}_m = \boldsymbol{f} \tag{2}$$

Efficient iterative solvers[17] are often used to solve Eq. (2), so that the matrix inverse might never be explicitly calculated. Even so, the number of frequency samples is usually still much smaller than the number required to obtain accurate response estimates in the band by polynomial-based interpolations. The problem is now simply stated as follows: given the matrices $\boldsymbol{K}$ and $\boldsymbol{M}$ and the response vectors $\boldsymbol{x}_m$ in Eq. (2), efficiently estimate the response vector $\boldsymbol{x}(\lambda)$ for λ in the band $\lambda_{\min} \le \lambda \le \lambda_{\max}$. Implicit in this problem statement is the need to understand errors in the estimates.

Forced-Response Condensation

In the present work the term *condensation* refers to a process of condensing out the degrees of freedom that are most important to predicting the forced response. This section begins with an analysis that motivates the choice of forced-response vectors for the condensation, proceeds with an analytical description of the condensation, and concludes with an algorithm for its implementation.

Motivation

To motivate the approach, we consider the modal expansion of a forced-response vector, which is a solution to Eq. (1):

$$\boldsymbol{x}(\lambda) = \sum_{n=1}^{N} \frac{\boldsymbol{\phi}_n\boldsymbol{\phi}_n^T}{\lambda_n - \lambda}\boldsymbol{f} \tag{3}$$

Here $(\lambda_n, \boldsymbol{\phi}_n)$ is the eigenpair that satisfies the generalized eigenvalue problem

$$(\boldsymbol{K} - \lambda_n\boldsymbol{M})\boldsymbol{\phi}_n = 0 \tag{4}$$

The eigenvectors are mass normalized according to

$$\boldsymbol{\phi}_n^T\boldsymbol{M}\boldsymbol{\phi}_n = 1 \tag{5}$$

The eigenpairs are divided into lower, interior, and upper groups according to whether the eigenvalue is below, inside, or above the band of interest. To identify the groups, the following sets of indices are defined:

$$n \in l \quad \text{for} \quad \lambda_n < \lambda_{\min} \tag{6}$$

$$n \in i \quad \text{for} \quad \lambda_{\min} \le \lambda_n \le \lambda_{\max} \tag{7}$$

$$n \in u \quad \text{for} \quad \lambda_n > \lambda_{\max} \tag{8}$$

This allows Eq. (3) to be expanded to

$$\boldsymbol{x}(\lambda) = \Sigma\boldsymbol{x}_l(\lambda) + \Sigma\boldsymbol{x}_i(\lambda) + \Sigma\boldsymbol{x}_u(\lambda) \tag{9}$$

where

$$\Sigma\boldsymbol{x}_q(\lambda) = \sum_{n \in q} \frac{\boldsymbol{\phi}_n\boldsymbol{\phi}_n^T}{\lambda_n - \lambda}\boldsymbol{f} \quad \text{for} \quad q = l, i, u \tag{10}$$

The contributions of the lower and upper eigenpairs in Eq. (9) vary smoothly as λ is varied in the band. However, the contributions of the interior eigenpairs approach infinity whenever λ approaches an interior eigenpair. If this frequency dependence is to be retained in the estimated responses, then the condensed equations should preserve the interior eigenpairs. The forced-response vectors defined in Eq. (2) hold great promise in achieving this because the small denominator in the interior term of Eq. (9) magnifies the contributions of the interior eigenpairs.

Description of Forced-Response Condensation

These considerations lead us to select the sampled response vectors in Eq. (2) as the basis set for the condensation. To condition the condensed problem numerically, we project the forced-response vectors onto a set of orthonormal vectors by a modified Gram–Schmidt procedure,[16] which leads to

$$\boldsymbol{X} = \boldsymbol{T}\boldsymbol{R} \tag{11}$$

where the M columns of $\boldsymbol{X}$ are forced-response vectors and the M columns of $\boldsymbol{T}$ are $\boldsymbol{M}$-orthonormal vectors. The upper triangular matrix $\boldsymbol{R}$ is $M \times M$. The procedure in Ref. 16 is extended to account for the $\boldsymbol{M}$-orthogonality requirement. The response vector at any frequency is approximated using the orthonormal basis

$$\boldsymbol{x}(\lambda) \approx \boldsymbol{T}\boldsymbol{y}(\lambda) \tag{12}$$

where $\boldsymbol{y}$ is a condensed vector of length M and $M \ll N$.

Substitution of Eq. (12) into Eq. (1) results in a residual vector $\boldsymbol{r}$ given by

$$\boldsymbol{r} = (\boldsymbol{K} - \lambda\boldsymbol{M})\boldsymbol{T}\boldsymbol{y}(\lambda) - \boldsymbol{f} \tag{13}$$

This residual is required to be orthogonal to the columns of $\boldsymbol{T}$, which simplifies Eq. (13) to

$$\boldsymbol{A}_T(\lambda)\boldsymbol{y}(\lambda) = (\boldsymbol{K}_T - \lambda\boldsymbol{I})\boldsymbol{y}(\lambda) = \boldsymbol{g} \tag{14}$$

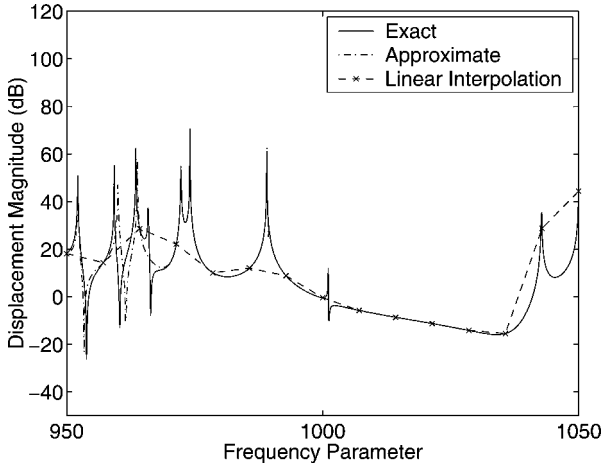

Fig. 1 Magnitude of response compared to an approximations from forced-response condensation and linear interpolation.

where $\boldsymbol{g} = \boldsymbol{T}^T\boldsymbol{f}$ and the condensed stiffness matrix is

$$\boldsymbol{K}_T = \boldsymbol{T}^T\boldsymbol{K}\boldsymbol{T} \tag{15}$$

Equation (14) can be solved for $\boldsymbol{y}(\lambda)$, which is substituted into Eq. (12) to yield an approximation $\tilde{\boldsymbol{x}}$ for $\boldsymbol{x}(\lambda)$:

$$\boldsymbol{x}(\lambda) \approx \tilde{\boldsymbol{x}}(\lambda) = \boldsymbol{T}\boldsymbol{A}_T^{-1}(\lambda)\boldsymbol{T}^T\boldsymbol{f} \tag{16}$$

Equation (16) provides the basic form of our interpolated or approximated response. Despite its apparent simplicity, it is capable of providing interpolated and/or estimated responses of surprisingly high accuracy. This is demonstrated in Fig. 1, which shows an exact response, a linearly interpolated response, and an approximation provided by Eq. (16). Over most of the range, the approximation overlaps the exact response. Details of the model are given in the Numerical Examples section. It is evident that the interpolation provided by Eq. (16) is superior to the simple linear interpolation. We note that the matrix $\boldsymbol{A}_T$ used to generate the interpolated response shown in Fig. 1 was only 15×15, and therefore its inverse is relatively easily computed. The basic forced-response condensation procedure is summarized in the following subsection.

Although the accuracy demonstrated in Fig. 1 is typical in our experience, it is not guaranteed. The main factors that affect the accuracy are the number of interpolation points in the frequency band of interest (relative to the number of natural frequencies in the band) and the accuracy of the approximate spectrum relative to the exact spectrum. These issues are described next, where precise error bounds on the spectrum are presented.

Direct numerical solution of Eq. (14) obscures errors introduced by the condensation. A much clearer framework for examining errors is obtained by computing the M eigenpairs $(\tilde{\lambda}_n, \tilde{\boldsymbol{\psi}}_n)$ of the condensed problem

$$(\boldsymbol{K}_T - \tilde{\lambda}_n\boldsymbol{I})\tilde{\boldsymbol{\psi}}_n = 0 \tag{17}$$

Using a modal expansion similar to Eq. (3) and the transformation in Eq. (12) yields an approximation of the full-response vector in terms of the condensed eigenpairs:

$$\tilde{\boldsymbol{x}}(\lambda) = \boldsymbol{T}\sum_{m=1}^{M}\frac{\tilde{\boldsymbol{\psi}}_n\tilde{\boldsymbol{\psi}}_n^T}{\tilde{\lambda}_n - \lambda}\boldsymbol{g} = \sum_{m=1}^{M}\frac{\tilde{\boldsymbol{\phi}}_n\tilde{\boldsymbol{\phi}}_n^T}{\tilde{\lambda}_n - \lambda}\boldsymbol{f} \tag{18}$$

Here, the expanded eigenvectors of the condensed model are given by $\tilde{\boldsymbol{\phi}}_n = \boldsymbol{T}\tilde{\boldsymbol{\psi}}_n$.

The condensed eigenpairs are grouped in the same way as the actual eigenpairs were in Eqs. (6–8):

$$n \in \tilde{l} \qquad \text{for} \qquad \tilde{\lambda}_n < \lambda_{\min} \tag{19}$$

$$n \in \tilde{i} \qquad \text{for} \qquad \lambda_{\min} \le \tilde{\lambda}_n \le \lambda_{\max} \tag{20}$$

$$n \in \tilde{u} \qquad \text{for} \qquad \tilde{\lambda}_n > \lambda_{\max} \tag{21}$$

The response in Eq. (18) is expanded as

$$\tilde{\boldsymbol{x}}(\lambda) = \Sigma\tilde{\boldsymbol{x}}_l(\lambda) + \Sigma\tilde{\boldsymbol{x}}_i(\lambda) + \Sigma\tilde{\boldsymbol{x}}_u(\lambda) \tag{22}$$

where

$$\Sigma\tilde{\boldsymbol{x}}_q(\lambda) = \sum_{n\in q}\frac{\tilde{\boldsymbol{\phi}}_n\tilde{\boldsymbol{\phi}}_n^T}{\tilde{\lambda}_n - \lambda}\boldsymbol{f} \qquad \text{for} \qquad q = \tilde{l},\ \tilde{i},\ \tilde{u} \tag{23}$$

We next consider errors in the approximated response in the interval $(\lambda_{\min}, \lambda_{\max})$. The exterior responses $\Sigma\tilde{\boldsymbol{x}}_l$ and $\Sigma\tilde{\boldsymbol{x}}_u$ do not contain singularities inside $(\lambda_{\min}, \lambda_{\max})$; however, the interior response $\Sigma\tilde{\boldsymbol{x}}_i$ approaches infinity as λ approaches an interior eigenvalue of the condensed model. As a result, the condensed interior eigenvalues must accurately approximate all of the actual interior eigenvalues if all of the peaks in $\tilde{\boldsymbol{x}}(\lambda)$ are to approximate those in $\boldsymbol{x}(\lambda)$ in the band of interest. This is not required of the exterior eigenpairs. Therefore, we shall analyze the interior and exterior responses separately in the following two sections. Following these sections, we apply results of Grimme[8] to the forced-response condensation and arrive at additional statements on its accuracy.

Basic Algorithm for Forced-Response Condensation

1) Compute M response vectors, $\boldsymbol{x}_m$, $m = 1, 2, \ldots, M$, satisfying Eq. (2).

2) Let $\boldsymbol{X} = [\boldsymbol{x}_1, \boldsymbol{x}_2, \ldots, \boldsymbol{x}_M]$. Use a modified Gram–Schmidt procedure[16] to compute the $\boldsymbol{M}$-orthonormal matrix $\boldsymbol{T}$ and upper triangular matrix $\boldsymbol{R}$ satisfying Eq. (11).

3) Compute $\boldsymbol{K}_T$ from Eq. (15) and $\boldsymbol{A}_T$ from Eq. (14).

4) Compute approximate response $\tilde{\boldsymbol{x}}$ from Eq. (16).

Remark: If Eq. (16) is to be evaluated many times for different values of λ, then it might be most efficient to compute $\boldsymbol{A}_T^{-1}(\lambda)$ using a spectral decomposition [see Eq. (18)].

Analysis of Interior Response

This section addresses two sources of errors in the interior responses. The first lies in the number of condensed interior eigenvalues. If this number is smaller than the number of actual interior eigenvalues, then peaks in the actual response will probably be completely missed in the condensed response. If this number is greater than the number of actual interior eigenvalues, then the condensed response might contain extra peaks that do not correspond to any actual peaks. The second source of error is caused by errors in the locations of the peaks themselves. As shown in Eqs. (10) and (23), the interior eigenvalues of the condensed problem must accurately approximate the interior eigenvalues of the full problem in order to get the peak location correct.

Expectation of Interior Eigenpair Accuracy

Before analyzing these errors in detail, we summarize an analysis that qualitatively indicates the conditions under which interior eigenpairs are preserved in the condensed model. A more complete form of this analysis can be found in a recent paper by McDaniel et al.[14] To begin, the matrix $\boldsymbol{X}$ of forced-response vectors is related to the matrix $\boldsymbol{\Phi}$ of eigenvectors by

$$\boldsymbol{X} = \boldsymbol{\Phi}\boldsymbol{C} \tag{24}$$

Each element of the modal amplitude matrix is identified from Eq. (3):

$$C_{mn} = \frac{\boldsymbol{\phi}_n^T\boldsymbol{f}}{\lambda_n - \sigma_m} \tag{25}$$

Little can be concluded from the numerator of C_{mn}, as the eigenvector is unknown. The denominator, however, is small (and C_{mn} is large) when λ_n is near σ_m. Therefore, amplitudes of the interior

eigenpairs are favored to be largest because the forced-response vectors are evaluated in the interior. Modal amplitudes of exterior eigenpairs can also be large because of either their proximity to the frequency band or to eigenvectors that are nearly parallel to the force vector.

Error Bounds for Eigenvalues

Errors in the interior condensed eigenvalues can be bounded by a variety of established analyses. We summarize some of them here. The simplest error bound can be found, among other places, in the text by Bathe.[18] For any orthonormal eigenvector estimate $\tilde{\boldsymbol{\phi}}_n$ and eigenvalue estimate $\tilde{\lambda}_n$, there is an actual eigenvalue λ_n that satisfies Eq. (1) and

$$\min_n |\tilde{\lambda}_n - \lambda_n| \leq \left\| \boldsymbol{M}^{-\frac{1}{2}} \boldsymbol{r}_M \right\|_2 = \sqrt{\boldsymbol{r}_M^T \boldsymbol{M}^{-1} \boldsymbol{r}_M} \tag{26}$$

where

$$\boldsymbol{r}_M = \boldsymbol{K}\tilde{\boldsymbol{\phi}}_n - \tilde{\lambda}_n \boldsymbol{M}\tilde{\boldsymbol{\phi}}_n \tag{27}$$

In the preceding equation and all that follow, it is implicitly assumed that the subscripts of an actual eigenvalue λ_n and its associated approximation $\tilde{\lambda}_n$ have been chosen to match.

Equation (26) defines a range on the λ axis in which the actual eigenvalue must lie, and this range will be referred to as a confidence interval. If the actual eigenvalues are tightly clustered, then the error bounds computed from Eq. (26) might be such that two or more confidence intervals overlap. The number of eigenvalues estimated by such a cluster of estimates is therefore uncertain. A theorem presented by Parlett[19] is useful in establishing a one-to-one correspondence between estimates and actual eigenvalues and in establishing confidence intervals for the estimates.

The theorem is presented by Parlett for the standard eigenvalue problem but is extended here to the generalized eigenvalue problem. To convert Eq. (4) to a symmetric standard form, we premultiply by $\boldsymbol{M}^{-1/2}$ and use the transformation $\boldsymbol{\phi}_n = \boldsymbol{M}^{-1/2}\boldsymbol{\psi}_n$ to get $(\boldsymbol{L} - \lambda \boldsymbol{I})\boldsymbol{\psi}_n = 0$, where $\boldsymbol{L} = \boldsymbol{M}^{-1/2}\boldsymbol{K}\boldsymbol{M}^{-1/2}$. The eigenvalues of the pencil $(\boldsymbol{K}, \boldsymbol{M})$ are equal to the eigenvalues of the pencil $(\boldsymbol{L}, \boldsymbol{I})$. Mass-orthonormal eigenvector estimates for all eigenpairs in the cluster are placed as columns in a matrix $\tilde{\boldsymbol{\Phi}}$. The theorem guarantees a one-to-one correspondence between the eigenvalue estimates $\tilde{\lambda}_n$ and the actual eigenvalues λ_n of the cluster, with the error bound

$$|\tilde{\lambda}_n - \lambda_n| \leq \|\boldsymbol{R}\|_2 \tag{28}$$

where $\boldsymbol{R} = \boldsymbol{L}\boldsymbol{Q} - \boldsymbol{Q}\boldsymbol{H}$ with $\boldsymbol{Q} = \boldsymbol{M}^{1/2}\tilde{\boldsymbol{\Phi}}$ and $\boldsymbol{H} = \boldsymbol{Q}^T\boldsymbol{L}\boldsymbol{Q}$. The spectral norm is defined by

$$\|\boldsymbol{R}\|_2 = \sqrt{\max\{\text{eig}(\boldsymbol{R}^T\boldsymbol{R})\}} \tag{29}$$

Because of the expense of computing $\boldsymbol{M}^{1/2}$, direct evaluation of Eq. (29) is inefficient. To overcome this, the orthonormality of the columns of $\tilde{\boldsymbol{\Phi}}$ is used to reduce $\boldsymbol{R}^T\boldsymbol{R}$ to

$$\boldsymbol{R}^T\boldsymbol{R} = \tilde{\boldsymbol{\Phi}}^T\boldsymbol{K}\boldsymbol{M}^{-1}\boldsymbol{K}\tilde{\boldsymbol{\Phi}} - \text{diag}(\tilde{\lambda}^2) \tag{30}$$

Counting Interior Eigenvalues

To determine whether all of the interior eigenvalues have been estimated, one must first determine the number of actual interior eigenvalues. This can be done by using a theorem,[19] which is based on the Sylvester law of inertia and requires the triangular factorization $\boldsymbol{K} - \sigma\boldsymbol{M} = \boldsymbol{L}_\sigma \boldsymbol{\Delta}_\sigma \boldsymbol{L}_\sigma^T$, where $\boldsymbol{\Delta}_\sigma$ is diagonal. If $\nu(\boldsymbol{A})$ is the number of negative eigenvalues of $\boldsymbol{A}$, then the theorem states that $\nu(\boldsymbol{K} - \sigma\boldsymbol{M}) = \nu(\boldsymbol{\Delta}_\sigma)$. The number of interior eigenvalues N_i is thus

$$N_i = \nu(\boldsymbol{K} - \lambda_{\max}\boldsymbol{M}) - \nu(\boldsymbol{K} - \lambda_{\min}\boldsymbol{M}) \tag{31}$$

The two triangular factorizations at $\lambda_{\min}$ and $\lambda_{\max}$ can be used to more efficiently calculate the forced responses at $\lambda_{\min}$ and $\lambda_{\max}$ if they are not yet available.

If a tolerance t_λ has been specified for the interior eigenvalues, then the set of accurate interior eigenvalues is defined for all condensed interior eigenvalues that satisfy $|\lambda_n - \tilde{\lambda}_n| \leq t_\lambda$. If the number of interior eigenvalues is greater than the number of accurate condensed eigenvalues in the interior, then singularities in the actual response might be missed by the condensed response. Depending on the application and available computer resources, one might wish to compute additional forced response vectors until all of the interior eigenvalues are approximated by the condensed eigenvalues.

Nonsymmetric Error Bounds

If all of the interior eigenvalues have been approximated, additional error information can be obtained. For all of the interior eigenvalues, we have bounds on the left and right neighboring eigenvalues. This information can be used to compute error bounds that are sometimes smaller than the bounds in Eq. (26) and Eq. (28). These bounds, which were presented by Crandall,[20] are given by

$$\tilde{\lambda}_n - \frac{Q - \tilde{\lambda}_n^2}{\lambda_{n+1} - \tilde{\lambda}_n} \leq \lambda_n \leq \tilde{\lambda}_n + \frac{Q - \tilde{\lambda}_n^2}{\tilde{\lambda}_n - \lambda_{n-1}} \tag{32}$$

where

$$Q = \frac{\left(\boldsymbol{M}^{-1}\boldsymbol{K}\tilde{\boldsymbol{\phi}}_n\right)^T \boldsymbol{M}\left(\boldsymbol{M}^{-1}\boldsymbol{K}\tilde{\boldsymbol{\phi}}_n\right)}{\tilde{\boldsymbol{\phi}}_n^T\boldsymbol{M}\tilde{\boldsymbol{\phi}}_n} = \frac{\tilde{\boldsymbol{\phi}}_n^T\boldsymbol{K}\boldsymbol{M}^{-1}\boldsymbol{K}\tilde{\boldsymbol{\phi}}_n}{\tilde{\boldsymbol{\phi}}_n^T\boldsymbol{M}\tilde{\boldsymbol{\phi}}_n} \tag{33}$$

Because the bound in Eq. (26) is symmetric about the approximate eigenvalue, it will be referred to as the symmetric bound to differentiate it from the nonsymmetric bound in Eq. (32).

To illustrate the differences in the bounds in Eqs. (26) and (32), they were compared for a variety of random systems in which the eigenvalues were known and the spacing was varied. In each system one eigenvalue was chosen as unity and the others were randomly selected with uniform distribution between 0 and 10. Each element of each eigenvector was randomly selected with normal distribution having zero mean and unity standard deviation. The mass and stiffness matrices were computed by

$$\boldsymbol{K} = \boldsymbol{\Phi}^{-T}\boldsymbol{\Lambda}\boldsymbol{\Phi}^{-1} \tag{34}$$

$$\boldsymbol{M} = \boldsymbol{\Phi}^{-T}\boldsymbol{\Phi}^{-1} \tag{35}$$

Estimates of the unity eigenvalue are obtained by computing a Rayleigh quotient with the approximate eigenvector found by randomly perturbing the exact one. The eigenvalue error bounds are plotted against the error in the eigenvalue estimate in Fig. 2. Here, the symmetric upper bound is tighter than the nonsymmetric one because of the proximity to unity of the nearest eigenvalue below unity. However, the nonsymmetric lower bound is tighter than the

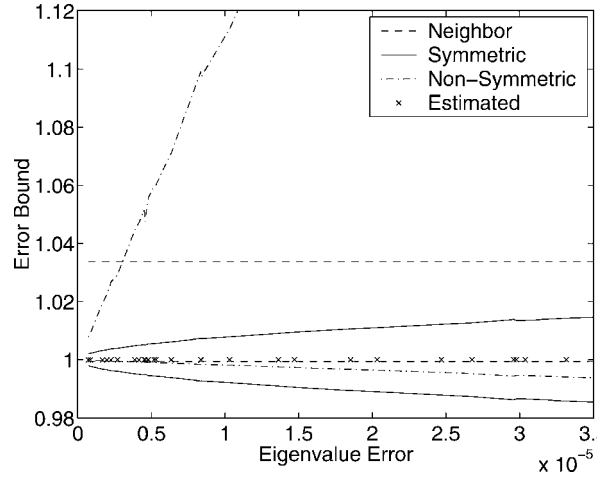

Fig. 2 Eigenvalue error bounds computed from Eqs. (26) and (32) for the unity eigenvalue.

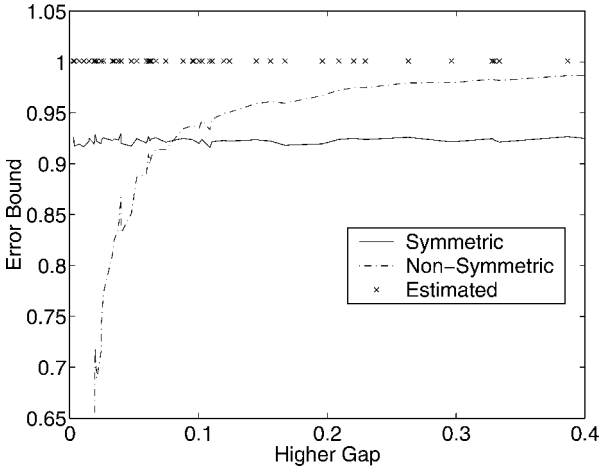

Fig. 3 Effect of nearest eigenvalue spacing on the eigenvalue error bounds computed from Eqs. (26) and (32) for the unity eigenvalue.

symmetric one because the nearest upper eigenvalue is farther from unity.

The effect of this proximity is more fully explored in Fig. 3, where the error bounds are plotted against the gap between unity and the closest eigenvalue below unity. These simulations use the same parameters as before, but in this case many realizations of the random system have been computed to allow examination of many gap sizes. As expected from Eq. (26), the symmetric bound is independent of the gap. However, the nonsymmetric bound is inversely proportional to the gap as expected from Eq. (32). For this particular problem, the nonsymmetric bound is tighter below a gap of approximately 0.05, whereas the symmetric bound is tighter above 0.05. Clearly, both bounds need to be considered in order to compute the tightest bound.

Application of Error Bounds

Our goal is to use the error bounds in Eqs. (26), (28), and (32) to obtain the smallest confidence interval for each of our interior eigenvalue estimates. In this section relationships between the error bounds are discussed, and a strategy is presented for applying them in concert. This strategy is formalized in two algorithms that are presented next.

The symmetric bounds in Eq. (26) are readily computable from a single eigenpair estimate, and so a natural first step is to compute confidence intervals for each interior eigenpair. If the confidence interval of a single eigenvalue does not intersect other confidence intervals, then the estimate is isolated, and one actual eigenvalue must lie in the interval. However, if two adjacent intervals overlap it can only be concluded that at least one actual eigenvalue lies in the union of the intersecting intervals.

For this reason eigenvalue estimates with intersecting confidence intervals are grouped into a cluster, and confidence intervals are recomputed using the cluster bounds in Eq. (28). It is possible that the newly computed interval will intersect a confidence interval of a neighboring cluster. If this happens, one must merge the overlapping intervals to form a new cluster and recompute the cluster bounds. This process continues until the confidence intervals of all clusters and isolated estimates are separated from each other.

If all of the eigenvalues in the band have been estimated, then the confidence intervals of isolated estimates can be reduced by evaluating the nonsymmetric bounds in Eq. (32). The reason for this condition is that one must have bounds on the neighboring eigenvalues, and this requires one to have estimates of the neighboring eigenvalues. For the inequality in Eq. (32) to prevail, we must use the maximum bound for the lower eigenvalue λ_{n-1} and the minimum bound for the higher eigenvalue λ_{n+1}. If the neighbor of an isolated estimate is also isolated, then the bounds for that neighbor should be recomputed first. This can be accomplished by computing the lower bound for the largest estimate first and proceeding to smaller estimates and by computing the upper bound of the smallest estimate first and proceeding to larger estimates. The upper bound of the smallest estimated eigenvalue can be computed by using $\lambda_{\min}$ as a bound for the nearest eigenvalue less than the smallest estimated eigenvalue. Similarly, the lower bound for the largest estimated eigenvalue can be computed using $\lambda_{\max}$. In the following two subsections two algorithms are presented for implementing these ideas:

Algorithm for Eigenvalue Error Analysis

1) For each interior eigenvalue estimate compute confidence intervals using the symmetric bounds in Eq. (26).

2) Repeat until no intervals overlap:

a) Merge isolated eigenvalue estimates or clusters with overlapping confidence intervals into clusters.

b) For each cluster compute new confidence intervals using Eq. (28) Consider one single confidence interval for each cluster.

3) Count the number of interior eigenvalues using Eq. (31), and compare to the number of estimated interior eigenvalues to determine if all interior eigenvalues have been estimated.

Algorithm for Improvement of Error Bounds for Isolated Estimates

1) Estimate all of the interior eigenvalues.

2) Identify the largest isolated estimate. For the identified estimate compute the lower bound according to the left-hand side of Eq. (32), using the lower bound of the larger estimate or $\lambda_{\max}$ for λ_{n+1}. Compare this bound to the one computed by the algorithm in the previous subsection. Select the largest lower bound.

3) Repeat the preceding step for the next smaller isolated estimate, proceeding sequentially until the smallest isolated interior estimate is reached.

4) Identify the smallest isolated estimate. For the identified estimate compute the upper bound according to the right-hand side of Eq. (32), using the upper bound of the smaller estimate for λ_{n-1}. Compare this bound to the one computed by the algorithm in the preceding subsection. Select the smallest upper bound.

5) Repeat the preceding step for the next larger isolated estimate, proceeding sequentially until the largest isolated interior estimate is reached.

Analysis of Exterior Response

By definition, neither the actual nor the condensed exterior response has singularities inside the band of interest. In our condensed model the exterior response is approximated by a small number of eigenpairs whose eigenvalues lie outside the band. In this section an analysis and two limiting cases are presented, which shed light on this process and give a qualitative description of the associated errors.

Collections of Exterior Eigenvalues

Effects of large collections of exterior eigenpairs on the response in a band can be approximated by a small number of eigenpairs in the condensed system. Here we present an analysis that shows the validity of this approximation. Consider a collection of eigenvalues defined by its center frequency λ_c and a set c of indices denoting the eigenpairs in the collection. The contribution of this collection to the response is

$$\boldsymbol{x}_c(\lambda) = \sum_{n \in c} \frac{\boldsymbol{\phi}_n^T \boldsymbol{f}}{\lambda_n - \lambda} \boldsymbol{\phi}_n \tag{36}$$

By factoring $1/(\lambda_c - \lambda)$ and expanding the remaining λ dependence in a power series, we get

$$\boldsymbol{x}_c(\lambda) = \frac{1}{\lambda_c - \lambda} \sum_{n \in c} \left[\sum_{k=0}^{\infty} \left(\frac{\lambda_c - \lambda_n}{\lambda_c - \lambda} \right)^k \right] \boldsymbol{\phi}_n^T \boldsymbol{f} \boldsymbol{\phi}_n \tag{37}$$

If $|\lambda_c - \lambda_n| \ll |\lambda_c - \lambda|$ for each $n \in c$, then the power series can be approximated by its first term:

$$\boldsymbol{x}_c(\lambda) = \frac{1}{\lambda_c - \lambda} \sum_{n \in c} \boldsymbol{\phi}_n^T \boldsymbol{f} \boldsymbol{\phi}_n + \mathcal{O}\left(\frac{\lambda_c - \lambda_n}{\lambda_c - \lambda}\right) \tag{38}$$

In this limit the collection's λ dependence is that of a single eigenpair. This supports the notion that collections of exterior eigenpairs can be approximated by single eigenpairs in the condensed system.

Two Limiting Cases

If further assumptions are made on the distance of the collection from the frequency band, simpler results are obtained, which lead to physical insight into the effects of the collection on the response. Let us begin by examining the limit in which the collection is far below the frequency band, $\lambda_c \ll \lambda$. The response in Eq. (36) is approximated as

$$\boldsymbol{x}_c(\lambda) \approx \sum_{n \in c} \frac{\boldsymbol{\phi}_n^T \boldsymbol{f} \boldsymbol{\phi}_n}{-\lambda} = \frac{1}{-\lambda} \boldsymbol{M}_c^{\dagger} \boldsymbol{f} \tag{39}$$

where the inverse-mass matrix of the collection is

$$\boldsymbol{M}_c^{\dagger} = \sum_{n \in c} \boldsymbol{\phi}_n \boldsymbol{\phi}_n^T \tag{40}$$

In this limit the collection of eigenvalues dynamically behaves like a collection of masses, the values of which are contained in the collection mass matrix.

The opposite limit occurs when the collection is far above the frequency band, so that $\lambda_c \gg \lambda$, and Eq. (36) is approximated by

$$\boldsymbol{x}_c(\lambda) \approx \sum_{n \in c} \frac{\boldsymbol{\phi}_n^T \boldsymbol{f} \boldsymbol{\phi}_n}{\lambda_n} = \boldsymbol{K}_c^{\dagger} \boldsymbol{f} \tag{41}$$

where the inverse-stiffness matrix of the collection is

$$\boldsymbol{K}_c^{\dagger} = \sum_{n \in c} \frac{\boldsymbol{\phi}_n \boldsymbol{\phi}_n^T}{\lambda_n} \tag{42}$$

The collection is dynamically behaving like a collection of springs, the values of which are contained in the collection stiffness matrix.

Application of Moment-Matching Theorem to Total Response

For convenience of referral, the moment-matching theorem from Grimme is given in the Appendix. When applied to the proposed method, this theorem reveals that the approximation $\tilde{\boldsymbol{x}}$ matches the actual response $\boldsymbol{x}$ at the interpolations points. In addition, the value and first derivative of $\boldsymbol{x}^T \boldsymbol{f}$ matches at the interpolation points. In summary,

$$\tilde{\boldsymbol{x}}(\sigma_m) = \boldsymbol{x}(\sigma_m) \tag{43}$$

$$\frac{\mathrm{d}}{\mathrm{d}\lambda}\left[\tilde{\boldsymbol{x}}^T(\sigma_m)\boldsymbol{f}\right] = \frac{\mathrm{d}}{\mathrm{d}\lambda}\left[\boldsymbol{x}^T(\sigma_m)\boldsymbol{f}\right] \tag{44}$$

for $m = 1, 2, \ldots, M$.

Numerical Examples

The purpose of these examples is to illustrate properties of the forced-response condensation. All of the examples involve a system with $N = 100$. Each element of each eigenvector is randomly selected with normal distribution having zero mean and unity standard deviation. The frequency band of interest is defined by $\lambda_{\min} = 950$ and $\lambda_{\max} = 1050$. Ten eigenvalues are randomly placed in this band, 45 eigenvalues are randomly placed between 700 and 950, and 45 eigenvalues are randomly placed between 1050 and 1300. The mass and stiffness matrices are computed according to Eqs. (34) and (35) and held fixed for all of the results presented next. The force vector has unity for every element.

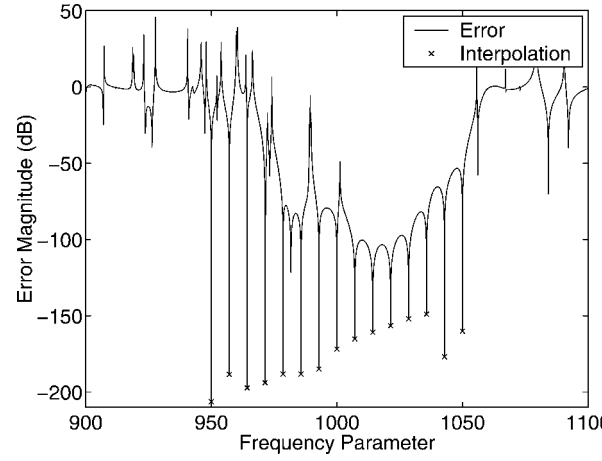

Fig. 4 Magnitude of error in the approximate response component in Fig. 1.

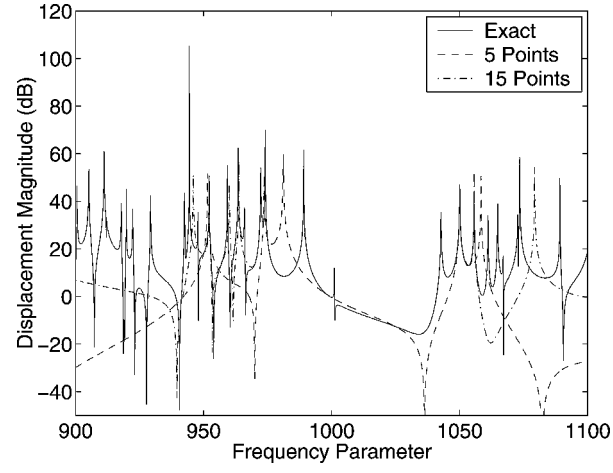

Fig. 5 Response magnitude compared to approximations from condensations with 5 and 15 response vectors.

The forced response is computed at 15 equidistant interpolation points σ_m, varying from $\lambda_{\min}$ to $\lambda_{\max}$. These 15 forced response vectors are used in the forced-response condensation method to generate the approximate forced response Eq. (18). The magnitude of the first component of the forced response and its approximation are plotted in Fig. 1. Note that the approximation response has peaks and valleys near those of the actual response in the band, indicating that the interior eigenvalues have been reasonably estimated. The magnitude of the corresponding error is plotted in Fig. 4. As discussed in Appendix, the interpolation matches the computed responses at the interpolation points. Another feature of the forced-response condensation, which is illustrated in this plot, is the local quality of the approximation, evidenced by the smaller errors in the band and the larger errors outside the band.

The effect of decreasing the number of interpolation points is illustrated in Fig. 5, where a condensation with five response vectors is compared to one with 15. Because the number of interpolation points is less than the number of interior eigenvalues, several peaks and valleys in the response are missed by the five-point model. The error magnitudes for the two approximations are compared in Fig. 6. Note that the five-point model has vanishing errors near the five interpolation points but generally has larger errors than the 15-point model as result of the missed interior eigenvalues.

The moment-matching theorem guarantees that the approximation matches the zeroth and first derivatives of the product $\boldsymbol{f}^T \boldsymbol{x}$ with respect to λ at the interpolation points. Because the force is known exactly, matching of the zeroth derivative has been demonstrated in the preceding results for response. The 15-point approximation for the first derivative is compared to the exact derivative in Fig. 7,

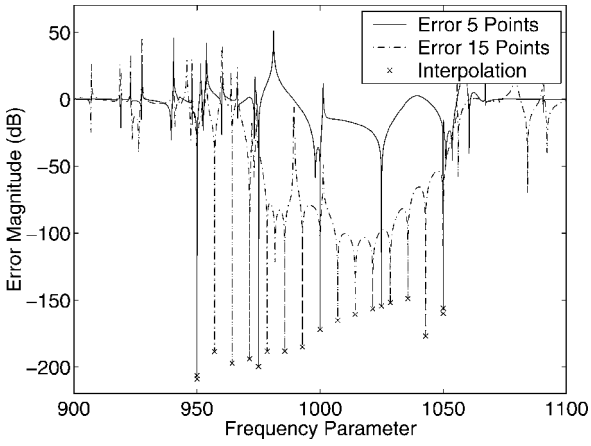

Fig. 6 Magnitude of error in the approximate response components in Fig. 5.

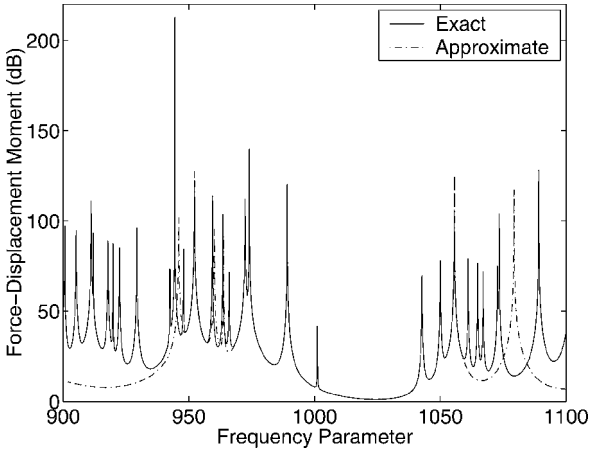

Fig. 7 First force-displacement moment $f^T x$ compared to an approximation from forced-response condensation.

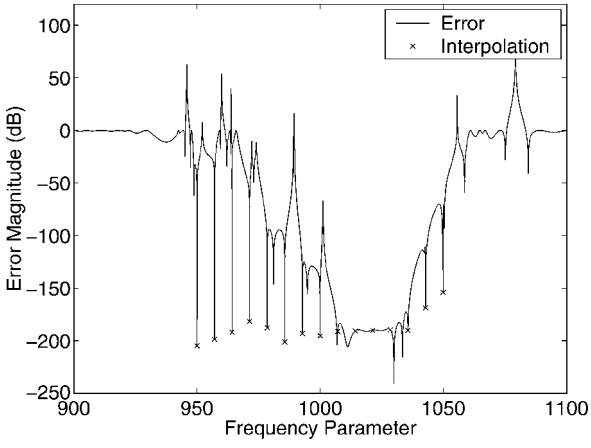

Fig. 8 Magnitude of error in the approximate force-displacement moment in Fig. 7.

where we again observe a matching of peaks and valleys. The error magnitude is shown in Fig. 8, where agreement is observed at the interpolation points.

Conclusions

The analysis presented here has demonstrated that one can develop an effective interpolation method that employs a relatively small set of forced response vectors in a dynamic condensation. This condensation favors retention of interior eigenpairs. The method approximates the in-band contributions of a potentially large number of exterior eigenpairs by a relatively small number of eigenpairs in the condensed model. The method is further distinguished by supporting analyses that indicate when the interior eigenspectrum is completely and accurately contained in the condensed model. Application of a moment-matching theorem from Grimme ensures that the response as well as the first two moments of the force-displacement product are exactly recovered at the interpolation points.

Several aspects of the method deserve future study. The examples presented here employ equally spaced interpolation points; however, better locations of the interpolation points would likely improve the method's accuracy. This possibility was suggested by the observation that interior eigenvalues near the ends of the band were more difficult to capture in the condensation. Relatively closer spacing of the interpolation points near the ends might remove this bias. One can also choose a new interpolation point based on the current condensations in an effort to improve the accuracies of the poorest eigenpair estimates.

Although the accuracy of the method has been assessed by examining errors in the interior eigenspectrum and by invoking the moment-matching theorem at interpolation points, error bounds on the dynamic response would be more useful in some situations. These bounds might be analytically derived by separately considering bounds on the interior and exterior responses. Bounds on the interior response would follow from error bounds on the interior eigenvalues and eigenvectors.

Appendix: Moment-Matching Theorem from Grimme

In this section we quote the moment-matching theorem from Grimme and relate it to the forced-response condensation Eq. (1). The theorem first appeared in the thesis by Grimme[8]; it can also be found in a paper by Gallivan et al.[12] A linear system with input $\boldsymbol{u}(t)$ and output $\boldsymbol{y}(t)$ is described by the state-space form

$$\begin{cases} \boldsymbol{E}\dot{\boldsymbol{x}}(t) = \boldsymbol{A}\boldsymbol{x}(t) + \boldsymbol{B}\boldsymbol{u}(t) \\ \boldsymbol{y}(t) = \boldsymbol{C}\boldsymbol{x}(t) + \boldsymbol{D}\boldsymbol{u}(t) \end{cases} \tag{A1}$$

and the reduced system is defined by

$$\begin{cases} \hat{\boldsymbol{E}}\dot{\hat{\boldsymbol{x}}}(t) = \hat{\boldsymbol{A}}\hat{\boldsymbol{x}}(t) + \hat{\boldsymbol{B}}\boldsymbol{u}(t) \\ \hat{\boldsymbol{y}}(t) = \hat{\boldsymbol{C}}\hat{\boldsymbol{x}}(t) + \hat{\boldsymbol{D}}\boldsymbol{u}(t) \end{cases} \tag{A2}$$

where the reduced matrices are $\hat{\boldsymbol{A}} = \boldsymbol{Z}^T\boldsymbol{A}\boldsymbol{V}$, $\hat{\boldsymbol{E}} = \boldsymbol{Z}^T\boldsymbol{E}\boldsymbol{V}$, $\hat{\boldsymbol{B}} = \boldsymbol{Z}^T\boldsymbol{B}$, $\hat{\boldsymbol{C}} = \boldsymbol{C}\boldsymbol{V}$, and $\hat{\boldsymbol{D}} = \boldsymbol{D}$.

The theorem states that if the following Krylov spaces are in the column spaces of the matrices $\boldsymbol{V}$ and $\boldsymbol{Z}$,

$$\bigcup_{k=1}^{K} \mathcal{K}_{J_{b_k}}\left\{\left[\sigma^{(k)}\boldsymbol{E} - \boldsymbol{A}\right]^{-1}\boldsymbol{E}, \left[\sigma^{(k)}\boldsymbol{E} - \boldsymbol{A}\right]^{-1}\boldsymbol{B}\right\} \subseteq \text{colsp}(\boldsymbol{V}) \tag{A3}$$

$$\bigcup_{k=1}^{K} \mathcal{K}_{J_{c_k}}\left\{\left[\sigma^{(k)}\boldsymbol{E} - \boldsymbol{A}\right]^{-T}\boldsymbol{E}^T, \left[\sigma^{(k)}\boldsymbol{E} - \boldsymbol{A}\right]^{-T}\boldsymbol{C}^T\right\} \subseteq \text{colsp}(\boldsymbol{Z}) \tag{A4}$$

then the moments of Eq. (45) and Eq. (46) satisfy

$$H_k^{(j_k)} = \boldsymbol{C}\left\{\left[\sigma^{(k)}\boldsymbol{E} - \boldsymbol{A}\right]^{-1}\boldsymbol{E}\right\}^{j_k - 1}\left[\sigma^{(k)}\boldsymbol{E} - \boldsymbol{A}\right]^{-1}\boldsymbol{B} \tag{A5}$$

$$= \hat{\boldsymbol{C}}\left\{\left[\sigma^{(k)}\hat{\boldsymbol{E}} - \hat{\boldsymbol{A}}\right]^{-1}\hat{\boldsymbol{E}}\right\}^{j_k - 1}\left[\sigma^{(k)}\hat{\boldsymbol{E}} - \hat{\boldsymbol{A}}\right]^{-1}\hat{\boldsymbol{B}} \tag{A6}$$

$$= \hat{H}_k^{(j_k)} \tag{A7}$$

for $j_k = 1, 2, \ldots, J_{b_k} + J_{c_k}$ and $k = 1, 2, \ldots, K$.

The theorem is applied to our system by transforming the governing equations in Eq. (1) to the frequency domain form of Eq. (45). The force is chosen as the input vector $\boldsymbol{B}$, and any unit vector can

be chosen as the output matrix $\boldsymbol{C}$ for the corresponding component of the forced response:

$$\begin{cases} \lambda \boldsymbol{M}\boldsymbol{x}(\lambda) = \boldsymbol{K}\boldsymbol{x}(\lambda) - \boldsymbol{f} \\ \boldsymbol{x}_m(\lambda) = \boldsymbol{e}_m^T \boldsymbol{x}(\lambda) \end{cases} \tag{A8}$$

The transformation matrix $\boldsymbol{T}$ defined by Eq. (11) is selected for $\boldsymbol{V}$. The columns of this matrix span the zeroth-order Krylov spaces of Eq. (47) corresponding to each interpolation point. The moment-matching theorem ensures agreement between any forced-response component at each interpolation point and its approximation. Furthermore, the theorem ensures that the component of the derivative of the forced response in the direction of the force vector is also matched. Indeed, if $\boldsymbol{f}$ is chosen for $\boldsymbol{C}$ the matrix $\boldsymbol{Z} = \boldsymbol{T}$ also spans the zeroth-order Krylov spaces of Eq. (A4). Two moments, the value and the derivative, of the function $p(\lambda) = \boldsymbol{f}^T \boldsymbol{x}(\lambda)$ are then matched at each interpolation point.

Acknowledgment

This material is based upon work supported by the National Science Foundation under Grants 9978747 and 9984994. The first author thanks Paul Van Dooren for having introduced him to Krylov projection methods during his teaching fellowship at the Université Catholique de Louvain.

References

[1]McDaniel, J. G., and Pierce, A. D., "Rational Interpolation of Sampled Frequency Response Calculations Based on Sophisticated Vibration Theory," *Proceedings of the American Society of Mechanical Engineers International Mechanical Engineering Congress and Exposition*, American Society of Mechanical Engineers, New York, 1998.

[2]Baker, G. A., and Graves-Morris, P. R., *Padé Approximants*, 2nd ed., Encyclopedia of Mathematics and Its Applications, Vol. 59, Cambridge Univ. Press, New York, 1996.

[3]Van Dooren, P., "Padé Approximations and the Lanczos Algorithm," *Short Course Benelux Meeting on Systems and Control*, 1995, URL: www.auto.ucl.ac.be/~vdooren/download/.

[4]Guyan, R. J., "Reduction of Stiffness and Mass Matrices," *AIAA Journal*, Vol. 3, 1965, p. 380.

[5]Flippen, L. D., Jr., "A Theory of Condensation Model Reduction," *Computers and Mathematical Applications*, Vol. 27, No. 27, 1994, pp. 9–40.

[6]Dyka, C. T., Ingel, R. P., and Flippen, L. D., "A New Approach to Dynamic Condensation for FEM," *Computers and Structures*, Vol. 61, No. 4, 1996, pp. 763–773.

[7]Ingel, R. P., Dyka, C. T., and Flippen, L. D., "Model Reduction and Frequency Windowing for Acoustic FEM Analysis," *Journal of Sound and Vibration*, Vol. 238, No. 2, 2000, pp. 327–350.

[8]Grimme, E., "Krylov Projection Methods for Model Reduction," Ph.D. Dissertation, Dept. of Electrical and Computer Engineering, Univ. of Illinois, Urbana, IL, May 1997.

[9]Freund, R. W., "Reduced-Order Modeling Techniques Based on Krylov Subspaces and Their Use in Circuit Simulation," *Applied and Computational Control, Signals, and Circuits*, Vol. 1, 1999, pp. 435–498.

[10]Freund, R. W., "Passive Reduced-Order Modeling via Krylov-Subspace Methods," *Proceedings of the 14th International Symposium on Mathematical Theory of Networks and Systems (MTNS 2000)*, Perpignan, France, June 2000.

[11]Grimme, E., Gallivan, K. A., and Van Dooren, P. M., "On Some Recent Developments in Projection-Based Model Reduction," *ENUMATH 97 (Heidelberg)*, World Scientific Publishing, River Edge, NJ, 1998, pp. 98–113.

[12]Gallivan, K., Grimme, E., and Van Dooren, P., "Model Reduction of Large-Scale Systems: Rational Krylov Versus Balancing Techniques," *Error Control and Adaptivity in Scientific Computing*, edited by H. Bulgak and C. Zenger, C-536, Kluwer Academic, Dordrecht, The Netherlands, 1999, pp. 177–190.

[13]Penzl, T., "Algorithms for Model Reduction of Large Dynamical Systems," TU Chemnitz, TR SFB393/99-40, Chemnitz, Germany, 1999, URL: http://www.tu-chemnitz.de/sfb393/sfb99pr.html.

[14]McDaniel, J. G., Widjaja, F., Barbone, P. E., and Pierce, A. D., "Estimating Natural Frequencies and Mode Shapes from Forced Response Calculations," *AIAA Journal*, Vol. 40, No. 4, 2002, pp. 758–764.

[15]Ruhe, A., "Rational Krylov, a Practical Algorithm for Large Sparse Nonsymmetric Matrix Pencils," *SIAM Journal on Scientific Computing*, Vol. 19, No. 5, 1998, pp. 1535–1551.

[16]Golub, G. H., and Van Loan, C. F., *Matrix Computations*, 3rd ed., Johns Hopkins Univ. Press, Baltimore, MD, 1996, pp. 231, 232 403, 404.

[17]Wu, K., and Milne, B., "A Survey of Packages for Large Linear Systems," Lawrence Berkeley National Lab., Rept. LBNL-45446, Berkeley, CA, Feb. 2000.

[18]Bathe, K.-J., *Finite Element Procedures*, Prentice–Hall, Upper Saddle River, NJ, 1996, Sec. 10.4.

[19]Parlett, B. N., *The Symmetric Eigenvalue Problem*, Classics in Applied Mathematics, Society for Industrial and Applied Mathematics, Philadelphia, 1998, Theorems 3.3.1 and 11.5.1.

[20]Crandall, S. H., *Engineering Analysis, A Survey of Numerical Procedures*, Engineering Societies Monographs, McGraw–Hill, New York, 1956, p. 115.

A. Berman
Associate Editor